Available online at www.sciencedirect.com
SCIENCE DIRECT®
Thermochimica Acta 432 (2005) 127–134
thermochimica acta
www.elsevier.com/locate/tca

The influence of the surface on the thermodynamics of the melting and glass transition of films and fibers☆,☆☆

Bernhard Wunderlich[a, b, *]

[a] *Department of Chemistry, University of Tennessee, Knoxville, TN 37996-1600, USA*
[b] *Chemical Sciences Division, Oak Ridge National Laboratory, Oak Ridge, TN 37831-6197, USA*

Received 20 October 2004; received in revised form 2 January 2005; accepted 3 January 2005
Available online 5 February 2005

Abstract

The influence of the surface on the thermodynamics of the melting and glass transition of films and fibers is negligible as long as the dimension of the phase is macroscopic, i.e., is more than 1 μm in all directions. The influence of the surface on microphases was discovered at the beginning of the 20th century, and is presently developing into the central topic for the description of hard and soft nanophase materials. The central issues of the thermal analysis of films and fibers, thus, are: the assessment of small sample masses, the evaluation of the nature of the surface, the treatment of irreversible phase structures, and the use of fast measurements to avoid reorganization of the metastable material without loss of precision. A short history of the roots of calorimetry of such small systems is used to arrive at a thermodynamic description of linear macromolecules in the amorphous state and, when partially crystallized, in the macroscopic, globally metastable structure which consists of multiple nanophases.
© 2005 Elsevier B.V. All rights reserved.

Keywords: Nanophase; Microphase; Polymer; Nonequilibrium thermodynamics; Glass transition; Melting; Rigid–amorphous fraction; Surface; Calorimetry; Film; Fiber; Gibbs–Thomson equation

1. Introduction

Over the past 14 years the continuous progress in calorimetry has been discussed at the Lähnwitz Seminars [1]. Since 1996, the topics developed in a continuous progression from the description of temperature-modulated calorimetry (TMC), to the treatment of phase transitions by TMC and the frequency and time dependence of heat capacity, C_p, to thermodynamics of small systems, to lead in 2004 to the calorimetry of thin films [2].

In this paper it is shown that knowledge about the thermodynamics and calorimetry of thin films dates back many years [3,4], that macromolecules do not form equilibrium crystals, and that subsequent annealing only rarely reaches equilibrium [5]. Irreversible thermodynamics allows in some cases to use the Gibbs–Thomson equation for the description of melting of thin, crystalline lamellae [6]. For further understanding of the defects in polymer crystals, the atomic details of surfaces, and crystal defects could be modeled by large-scale molecular dynamics simulation [7]. These can then be extended by coarse-grain Monte Carlo simulations to macroscopic dimensions and time scales [8]. Other observations related to this topic deal with the changes of crystal morphology encountered on volume restriction [9], the introduction of surface strain as in rigid–amorphous fractions, RAF [10], and changes in phase transitions of single [11] and

☆ Presented at the Eighth Lähnwitz Seminar on "Thermodynamics and Calorimetry of Thin Films," 7–10 June 2004.

☆☆ This manuscript has been authored by a contractor of the U.S. Government under the contract No. DOE-AC05-00OR22725. Accordingly, the U.S. Government retains a non-exclusive, royalty-free license to publish or reproduce the published form of this contribution, or allow others to do so, for U.S. Government purposes.

* Tel.: +1 865 675 4532; fax: +1 865 675 4532.
E-mail address: wunderlich@chartertn.net.

0040-6031/$ – see front matter © 2005 Elsevier B.V. All rights reserved.
doi:10.1016/j.tca.2005.01.010

multiple layers of molecules on solid surfaces [12]. In drawn fibers and films, finally, the RAF may be oriented and can affect the mechanical properties [13]. The topics just listed are discussed in this paper.

2. Thermodynamics of thin films

The problems of calorimetry of macromolecules in small systems were discussed at the Seventh Lähnwitz Seminar [2,14]. The key issue in [14] was the separation of macrophases, microphases, and nanophases. Little of all matter, and perhaps even none, is in equilibrium. The early efforts to find descriptions of thermal processes, thus, faced great difficulties due to the encountered metastable states. Progress was made with the development of equilibrium thermodynamics at the end of the 19th century. Equilibrium is a limiting state, described by the functions of the second law, as given by free enthalpy, G, for the characterization of stability, and entropy, S, as a measure of the degree of disorder. Both functions being linked to the first-law enthalpy, H. Basic to the description of equilibrium was the definition of a phase as a state of matter that is uniform throughout, not only in chemical composition, but also in physical state. In other words, a macrophase consists of a homogeneous volume of matter, separated by well-defined surfaces of negligible influence on the phase properties [15].

As the phase dimensions decrease to the micrometer level, the surface free energy is not negligible, as demonstrated by Meissner in 1920 [4]. The melting temperatures of some organic materials, such as azobenzene and tristearin decreased by about 0.4 K for a decrease in thickness from 10 to 0.8 μm, as is illustrated by Fig. 1 which is based on the original publication. A cylindrical lens was pressed with its long axis parallel to a temperature gradient, produced by the two constant temperature baths at the ends of the polished iron support. The changing thickness of the crystal could be calculated from the position of the lens, measured by interference fringes. Surprisingly, some other samples, such as *p*-chloroanilin and stearic acid showed no change in melting temperature. One may assume, in hindsight, that these samples were microcrystalline and, as such, are independent of a restraining volume of larger size. The Gibbs–Thomson equation, as given in the figure, was used to derive the specific surface free energy, σ, from the experiment. Note that ΔT ($=T_m^0 - T$) is the ratio of σ to the entropy ($\Delta h_f/T_m^0$) with a geometric factor $\updownarrow/2$, where Δh_f is the specific heat of fusion, ρ the crystal density, and $\updownarrow$, the crystal thickness.

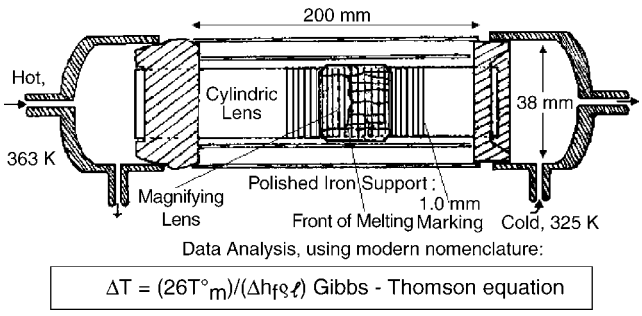

Fig. 1. Copy of a schematic of the experimental set-up for the measurement of the melting temperature of thin crystals, as developed in the 1920s [4].

As soon as the morphology of polymer crystals was identified as lamellar, with common thicknesses from 5 to 50 nm, the Gibbs–Thomson equation was used for the analysis of the melting temperature [6], as shown in Fig. 2 [16]. Data from several laboratories are combined in this figure. The crystal thicknesses as evaluated in most cases from low-angle X-ray diffraction and interference microscopy. The least-squares equation in Fig. 2 is well within the error limit and suggests that lamellar microcrystals with few internal defects can be described with one additional, internal thermodynamic parameter, the surface free energy, σ.

Adding one more step in the decrease of phase dimension leads to nanophases. The definition of a nanophase was linked to the absence of bulk phase between the surfaces of a film, i.e., the effects of one surface reaches to the opposing one [14]. The limits of the size of a nanophase will change with type of material. The lower limit is, as already assumed for the macrophase, the need of a homogeneous material. As soon as the atomic dimensions come into play, a thermodynamic description of the nanophase becomes impossible and the phase concept becomes inapplicable. Matter of such dimensions must be described as clusters of atoms or molecules, rather than phases. Early experiments are reproduced in Fig. 3 for the change of melting temperature of argon, adsorbed on TiO_2 [17]. The amount of adsorbed argon was determined by the change in pressure of the applied volume (BET method). The initial decrease in melting temperature can still be approximated by assuming the presence of a microphase. The thinner layers, however, show no sharp melting, they are nanophases. A recent analysis by AFM of long-chain paraffins ($C_{390}H_{782}$) adsorbed on crystalline graphite revealed that

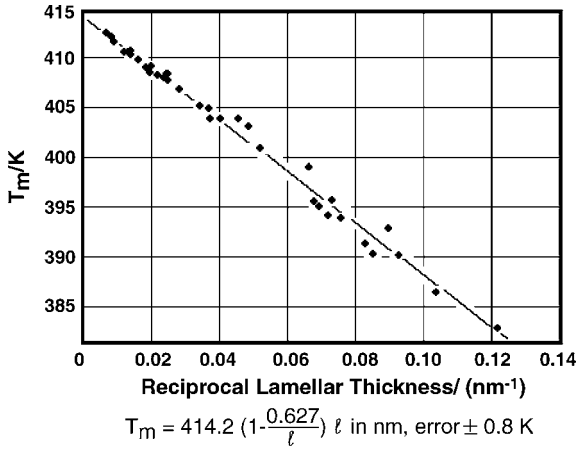

Fig. 2. Change of the melting temperature of polyethylene lamellae as a function of thickness, ℓ represented by data collected from the literature in [16] (vol. 3, Fig. VIII.10).

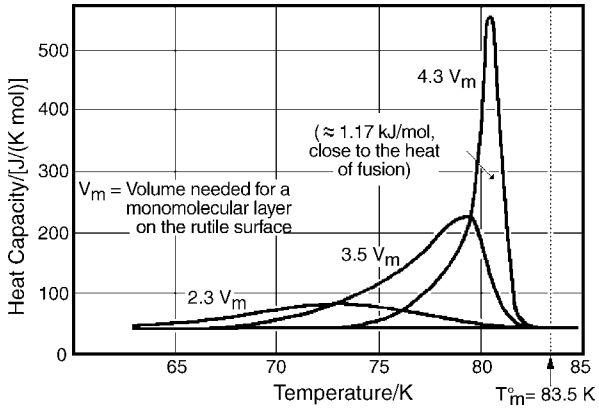

Fig. 3. Change of the melting characteristic of argon as a function of absorbed layer thickness on TiO_2, as measured by the partial molar heat capacity. Drawn from data reported in [12].

ordered monomolecular layers could exist *above* the melting temperature of the single crystals (≈400 K) [11]. These ordered monomolecular layers show a change in morphology (between 433 and 443 K) and randomize (melt) only above 463 K. In this case it is to be assumed that the interfacial free energy causes the stability of the nanophase. This observation may also explain why paraffins and polyethylene in contact with various solid surfaces need no crystal nucleation, but supercool when in microphase droplets [18,19]. The ordered monomolecular film of adsorbed paraffin could easily serve as a crystal nucleus.

The behavior of thin films of amorphous polymers was addressed by studies of the glass transition of spheres of polystyrene and of block copolymers with a lamellar superstructure [20]. The broadening of the glass transition of the free-standing spheres of polystyrene could be linked to a 5 nm thick surface layer with continuously lower glass transition as the surface was approached, reaching ultimately a lowering of about 40 K. This observation indicates that free-standing films of less than 10 nm thickness should not show any residual bulk glass transition of 373 K. The layers of the block copolymers produce a similar broadening of the glass transition to lower temperatures in case the neighboring phase is more mobile, and to higher temperature if the neighboring phase is glassy, as shown in Fig. 4. Details about this nanophase property were discussed at the Seventh Lähnwitz Seminar [14]. Similar conclusions were reached more recently, based on model calculations and Brillouin light scattering data on thin, free-standing films of polystyrene down to a thickness of 20 nm [21]. Surprisingly, thin-film chip calorimetry [22] of polystyrene on very fast heating and cooling down to 15 nm showed no influence on glass transition temperature [23]. The main question in these seemingly contradictory results is the effect of the remaining interface of the polystyrene to the silicon nitride which is its support in the chip calorimeter. It is also of interest, to note that while the analysis of the polystyrene beads showed in the vicinity of the glass transition a strong exotherm due to the coalescence of the microphase beads to a macroscopic droplet, there was no

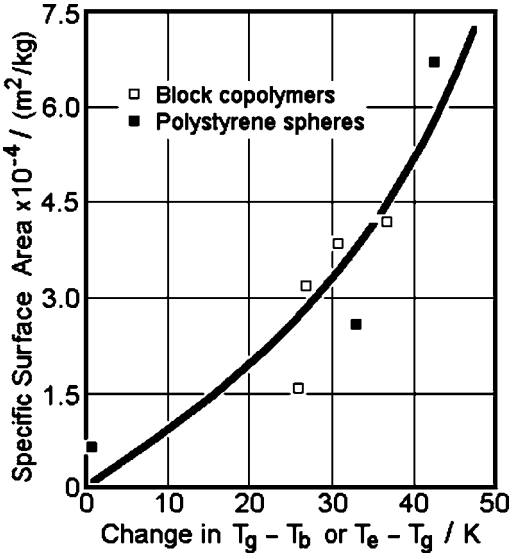

Fig. 4. Changes of the glass transitions with increasing specific surface area of the phase of lamellarly separated block copolymers of polystyrene and poly(α-methyl styrene) and small spheres of polystyrene [21]; (T_b is the beginning of the glass transition and T_e, the end, while T_g is taken at the point where half of the change of the heat capacity has occurred).

similar exotherm seen in the fast chip-calorimetry, perhaps indicating no reduction of the surface free energy due to the influence of the silicon nitride support film.

3. Crystallization in thin films

Droplets of single molecules of amorphous, high-molar-mass isotactic polystyrene where produced by deposition of a dilute solution in benzene on a water surface by the Langmuir method and transfer to an electron-microscopy support. These droplets were then crystallized at 448.2 K for 8 h and yielded single-molecule single-crystals, as shown in Fig. 5 [24]. The crystals are lamellar, single-molecule microphases, as proven by electron diffraction. The shape did not reach the

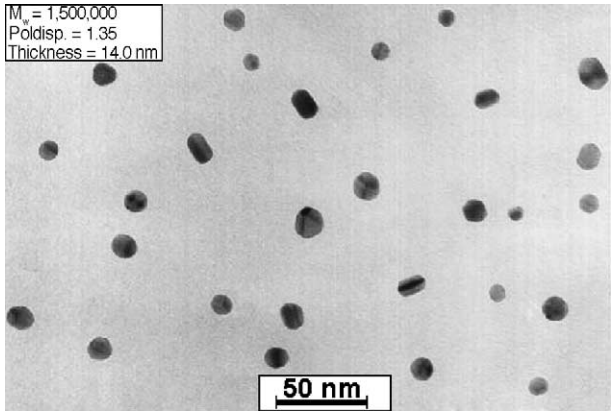

Fig. 5. Electron micrograph of single-molecule single-crystals of isotactic polystyrene, illustrating that single molecules do not reach the equilibrium morphology on initial crystallization [24].

equilibrium dimensions as expected for the habit of minimum free-enthalpy using the appropriate specific surface free energies. This experiment is in accord with the chain-folding principle [16] and suggests that this principle extends to single-molecule, microphase volumes. Only when the size of the molecule restricts the crystal to smaller dimensions is greater metastability expected. Also, it is of interest to note that the molecular chains are normal to the substrate, an orientation that is also observed in films of poly(oxyethylene) produced by pseudo-dewetting of thin films on silicon wafers, followed by crystallization [8]. In epitaxy on most surfaces, in contrast, the chains lie in the plane of the substrate [16], which may have its origin in true monomolecular layers serving as a crystal nucleus, as observed with paraffins [11].

The effect of external restrictions on the crystallization of poly(oxyethylene) retained in lamellar spaces of glassy polystyrene within a poly(oxyethylene-*block*-styrene) is illustrated in [9]. On cooling from the liquid solution of the block copolymer, one observes at 433 K a microphase separation of the blocks of the copolymer into a lamellar superstructure with 8.8 nm thick layers of liquid poly(oxyethylene) and 9.9 nm polystyrene. The junctions between the blocks of the copolymer are located at the lamellar interfaces and serve as points of decoupling. At 335 K, about 30 K below the expected T_g of the bulk phase of the same molar mass, the glass transition of the polystyrene leads to alternating solid polystyrene and liquid poly(oxyethylene) layers. Note that the lowering of T_g due to the created specific surface area agrees with Fig. 4. Below 324 K, the poly(oxyethylene) can crystallize. As shown in the schematic of Fig. 6, at low temperature, the fold length and lateral extension of the crystals is sufficiently small to result in a random orientation of the crystals. At higher temperatures, larger, more perfect crystals grow and are forced to orient. First, they align with their growth-faces parallel to the lamellar surface, and then at right angles, finally producing the most stable crystals permitted by the glassy structure of the polystyrene. Crystallizing such block copolymers from a common solvent, the solidification of polystyrene at T_g is circumvented, and phase separation is driven by the crystallization of the poly(oxyethylene) blocks, causing the bottom morphology in Fig. 6 with laterally macroscopic single crystals [24].

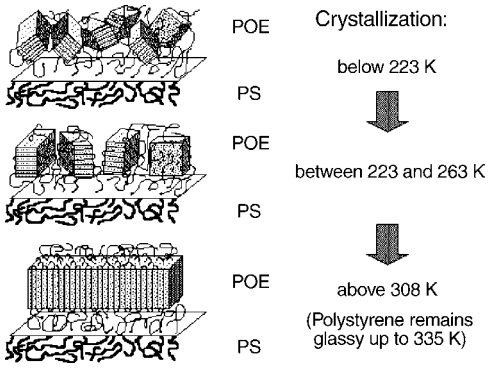

Fig. 6. Orientation of poly(oxyethylene) crystals (POE) contained in a lamellar block-copolymer structure between layers of glassy polystyrene blocks (PS). Molar mass of the POE blocks = 8.7 kDa, of the PS blocks = 9.2 kDa [9].

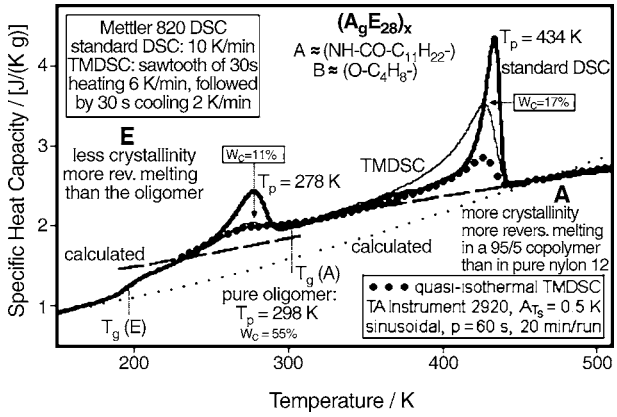

Fig. 7. Temperature-modulated and standard DSC of a multiblock copolymer of oligoamide 12 (A) and oligooxytetramethylene (E) sequences [25].

A greater influence on the crystallization is exerted when the blocks of a copolymer become even shorter than in Fig. 6. In this case the crystallinity and melting temperatures are reduced, as was documented with multi-block copolymers of oligoamide 12 and oligooxytetramethylene, displayed in Fig. 7 [25]. The influence of the solid oligoamide 12 reduces the crystallinity of the oligooxytetramethylene, while at a sufficiently high concentration of oligoamide 12 (weight ratio 95/5), its crystallinity increases relative to the homopolymer due to a higher mobility introduced by the comonomer. These observations point to the influence of strain across the interface.

4. Strain-effects across interfaces of crystals

A general observation for semicrystalline polymers is the broadening of the glass transition to higher temperature. This must mean, that a portion of the non-crystalline material has become less mobile. In fact, this loss of mobility is the main reason for polymers to stop crystallization before reaching a crystallinity of 100%. On cooling below T_m, the bulk-amorphous free enthalpy of crystallization ($G_{crystal} - G_{amorphous}$) becomes more negative, indicating an increasing thermo dynamic driving force toward crystallization. As, however, crystallization progresses, the increasing strain transmitted by the tie molecules between the crystals and the neighboring amorphous phase renders the global structure metastable in a semicrystalline nanophase-separated state.

A more detailed observation of strained nanophase structures in semicrystalline polymers is possible in drawn polymers because of possible ordering, detectable by X-ray diffraction. Such analysis was first shown for fibers of poly(ethylene terephthalate) by a full-pattern analysis (Rietvelt analysis). An oriented mesophase could be

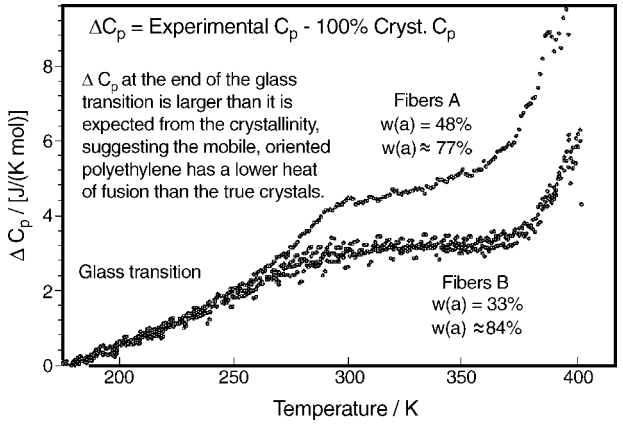

Fig. 8. Increase in heat capacity with temperature in the glass-transition region of gel-spun polyethylene of ultra-high molar mass [26]. For the macroscopic, amorphous phase of polyethylene the glass transition temperature is 237 K, and the transition is completed at 250 K.

identified which governed the mechanical properties of the semicrystalline fibers [13]. In Fig. 8, such strain between crystals and amorphous material is documented by thermal analysis for the case of gel-spun, ultra-high-molar-mass polyethylene [26]. Not only is in this case the glass transition spread to higher temperature, but the sum of the percentage amorphous calculated from ΔC_p at T_g and the crystallinity from the heat of fusion is more than 100%. This proves that at room temperature a degree of orientation exists in the noncrystalline fraction which contributes a heat of disordering when the crystals melt and the strain is released, i.e., the heat of fusion measured is more than expected from the crystals alone. The existence of partial order with limited mobility, larger than in the crystal and less than in the melt, could furthermore be proven by solid-state NMR and X-ray diffraction [13].

In undrawn samples, the broadened glass transition is the primary evidence for strain caused by decoupling of parts of the molecules at the phase boundary. In Fig. 9, on the left, the analysis of the heat capacity, C_p, of poly(oxymethylene) reveals a measured C_p which is smaller than calculated from crystallinity [10]. The resulting ΔC_p at T_g versus the heat of fusion in the graph on the right of Fig. 9 illustrates the interpretation of this heat-capacity decrement as a rigid–amorphous fraction (RAF). The RAF indicates the presence of a third phase which is not in equilibrium, complicating the overall structure of the polymer, as discussed in the Seventh Lähnwitz Seminar [14]. The measured C_p on the left in Fig. 9 indicates that the RAF of poly(oxymethylene) does not undergo a glass transition before the polymer melts, rather, on melting, the crystals and the RAF become mobile simultaneously.

Fig. 10 illustrates a detailed analysis of the heat capacity of poly(butylene terephthalate) as presented in [27]. Comparing the extrapolated heat capacities of the solid and liquid with the calculated values for different crystallinities, it is obvious that a first, broadened glass transition occurs between A and B with a ΔC_p of b–a, and the RAF has a separate glass transition between B and C with a ΔC_p of c–b at about 60 K higher temperature, just below the broad melting region from C to D. The crystallinity for this poly(butylene terephthalate) can be calculated down to 375 K with the common two-phase model, as is indicated by the equation in the figure.

A case where the glass transition of the RAF occurs *above* the melting transition is displayed in Fig. 11 for poly(oxy-2,6-dimethyl-1,4-phenylene) (PPO^{TM}) [28]. The standard DSC of this semicrystalline polymer of about 30% crystallinity shows no glass transition, but the polymer can be annealed below the melting peak and then develops a glass transition with a parallel decrease in crystallinity. The quasi-isothermal TMDSC data in Fig. 11 show that at increasing temperature the RAF decreases first from about 75% to 60% and then, at higher temperature this is followed by a parallel decrease of crystallinity and RAF. A detailed discussion of the RAF as a part of the overall phase-structure of semicrystalline polymers was given in [14]. It suggests that as a polymer approaches nanophase dimensions, the thermal properties change not only by size restrictions, as displayed in Section 2, but also by interactions with neighboring phases.

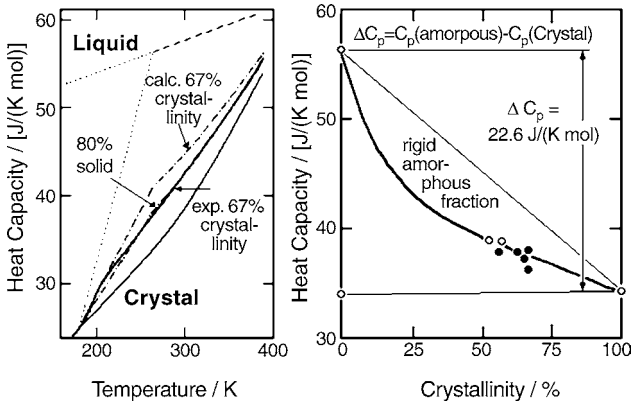

Fig. 9. Rigid–amorphous fractions and glass transition in poly(oxymethylene) [10].

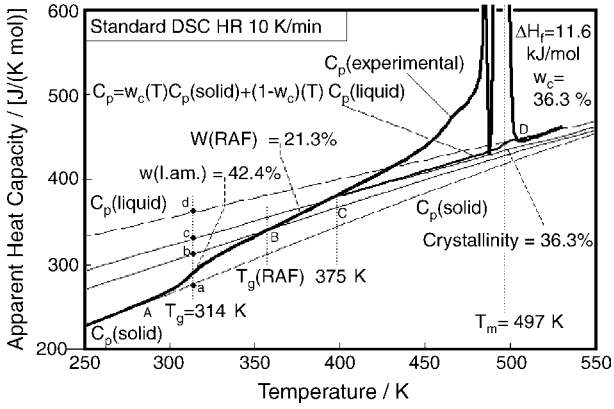

Fig. 10. Rigid–amorphous fractions and glass transitions in poly(butylene terephthalate) [27].

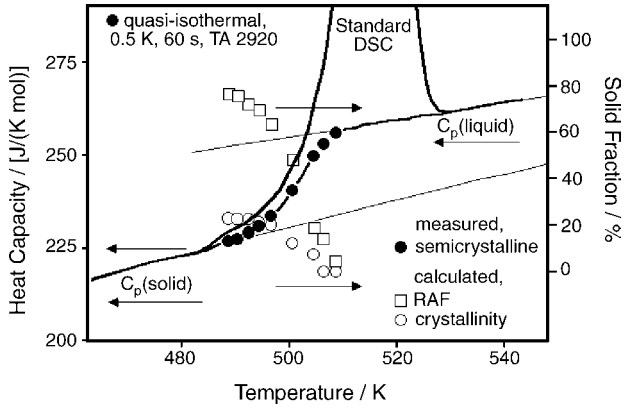

Fig. 11. Rigid–amorphous fractions and glass transitions in semicrystalline poly(oxy-2,6-dimethyl-1,4-phenylene) analyzed by standard and temperature-modulated DSC [28].

5. Thermal analysis of thin films

Based on the selection of experiments in Sections 2–4, thermal analysis of thin films and fibers must recognize their nonequilibrium character. The same is true for the bulk polymers since nanophases are prominent in these when dealing with semicrystalline polymers, block copolymers, and finely divided blends. The equilibrium thermodynamics of polymers was developed in the 1950s and 1960s [29] and today, it is still the dominant tool to analyze polymers [30]. But, over the years it has been proven increasingly deficient, it only represents the limit against which to judge the degree of metastability. In the following figures, nonequilibrium is described as it was developed in our laboratory to support quantitative thermal analysis [6,16,31]. As mentioned above, the roots of this description of small systems go back to the 19th century [15].

In Fig. 12, Eq. (1), the entropy is introduced as a function of time to follow irreversible processes. As is customary in the theory of irreversible thermodynamics [32], the total change in entropy is then separated into a *flux* (d $_eS$, for the external change) and a *production* (d $_iS$, for the internal change). The rate of flux and production of entropy have the dimension J K^{-1} s^{-1} and account for the changes per second. The *entropy flux*, may be caused by a heat-flow, dQ, across the system boundary and the flow of different types of matter, d $_en_i$, as shown in Eq. (2). This fluxes are the keys to thermal analysis. The heat-flow rate can be measured by DSC, and the changes in amount of matter within the system can be assessed by thermogravimetry, coupled, if need be, with mass spectrometry or GPC for identification of the matter exchanged. Any irreversible effects of the flux due to temperature and concentration gradients, which are needed to move heat and matter, are usually kept outside the system by maintaining the inside isothermal. Any remaining effects of gradients inside the system are made small by design of the thermal analysis experiment, and eliminated by calibration or the division into subsystems, as described below.

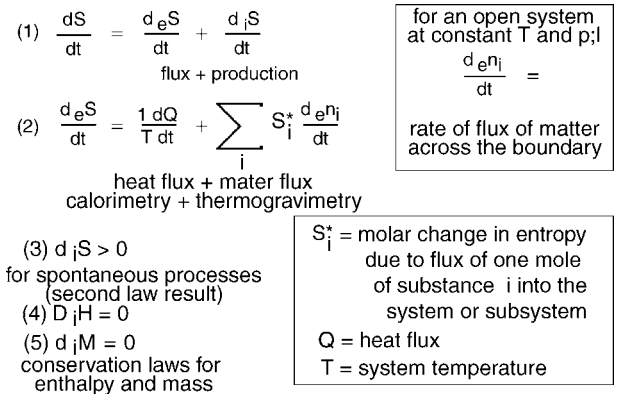

Fig. 12. Entropy flux and production. Analogous equations can be written for the extensive quantities enthalpy, H, and free enthalpy, G.

The *entropy production* is caused only by changes within the system. This production is governed by the conditions of the second and first law of thermodynamics, as given by Eqs. (3)–(5). By separating the flux in Eq. (1) from the global change, entropy production describes the system as if it were an *isolated system*. For isolated systems the second law requires that d $_iS = 0$ for equilibrium, and nonequilibrium, spontaneous processes are permitted as long as there is an entropy production, i.e., d $_iS > 0$. An entropy decrease is forbidden. Thus, the isolated system acts like a small universe in which entropy always increases or stays the same, but never decreases.

In order to apply this description to realistic situations, one must often subdivide the system into subsystems. Each subsystem is delineated such that it contains only negligible gradients in the intensive quantities such as temperature, pressure, and concentrations. If this is possible, each subsystem can be described as given in Fig. 12, and its changes can be separated into production and flux to and from the surrounding subsystems. Naturally, the number of quantities needed to be measured increases proportional to the number of subsystems required and becomes quickly an experimental nightmare. As soon as the subsystems become micro- or nanophases, surface free energies and deviations from the bulk properties must be included in the description. Ultimately, when the lower limit of the size of a nanophase is reached, no thermodynamic description is valid anymore because of the loss of homogeneity due to the molecular structure and the microscopic fluctuations in energy.

A system of interest to thermal analysis is described in Fig. 13. It consists of the sample, or in case of a standard DSC experiment, of the sample enclosed in a metal pan. This sample is divided into a crystalline and a melted subsystem. In such an arrangement the total system is a *closed system*, defined as a system that allows only flux of heat. In contrast to this closed system in DSC, thermogravimetry deals with *open systems* which allow flux of heat *and* matter. The description of melting and crystallization experiments by DSC in Fig. 13 also introduces an open interface between the crystalline and melted subsystem. Finally, one also can imagine

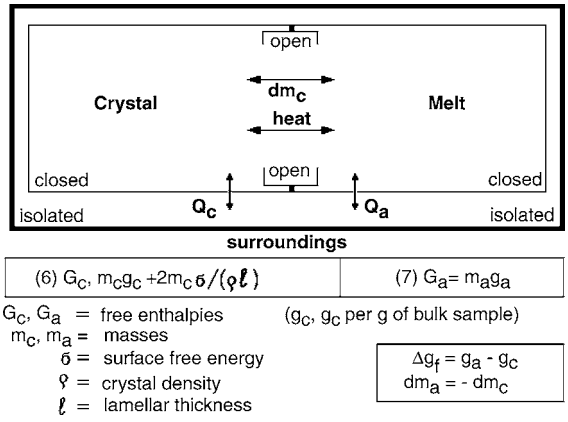

Fig. 13. Schematics of melting as it applies to a sample in a calorimeter. The subscripts 'a' and 'c' refer to amorphous and crystalline subsystems, and 'f' stand for fusion.

isolated systems, as mentioned above, systems without flux of any kind. The exchanged heat with the calorimeter as integral measurement is by Q_c and Q_a, the amounts that flows into the crystalline and amorphous subsystem, respectively. The crystals are assumed to all have the same lamellar shape and size, so that the surface effect of the crystals can easily be summed, as indicated in Eq. (6). A distribution of different lamellar sizes would be noticed by a melting-point distribution and could still be handled with a single DSC experiment. The melt is assumed to collect into a single system with negligible surface effect, as seen from Eq. (7). On melting, mass transport occurs across the open phase boundary between the two subsystems. The transition itself is driven by the heat flux to or from the calorimeter across the closed boundary, measured by the heat-flow rate. Relative to the surroundings, the overall calorimeter is isolated and at any instant essentially isothermal.

Finally, Fig. 14 summarizes the derivation of the Gibbs–Thomson equation (10), first mentioned in Fig. 1 for the description of the melting of thin films with a small ↕. For the assumed isothermal condition, the heat flux $dQ_c + dQ_a$ provides the latent heat, and determines the entropy flux into the sample when written as in Eq. (8). Heat capacity contributions need to be added as soon as the temperature of

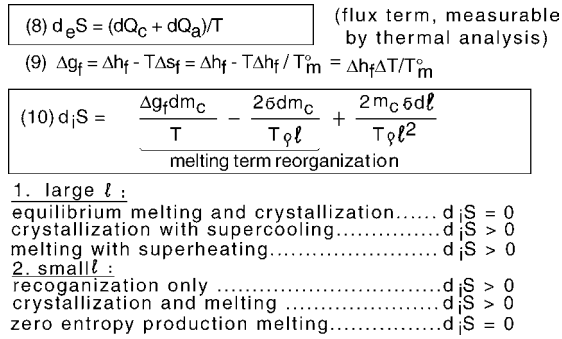

Fig. 14. Melting equation as derived from Figs. 12 and 13.

the system changes. Per gram of sample, the specific entropy production can also be written as $d_i s = (d_i h - d_i g)/T$, in $J\,K^{-1}\,g^{-1}$. This is simply $-d_i g/T$ because of the conservation in enthalpy for an isolated system, given by Eq. (4) in Fig. 12. The specific free enthalpy of fusion, Δg_f in $J\,g^{-1}$, is defined in Fig. 13, and developed in Fig. 14 by Eq. (9). For the melting of crystals, Δg_f indicates the metastability of the crystals and is given by the measured specific enthalpy of fusion, Δh_f, and the measured distance of T from the equilibrium melting temperature, T_m^0. The entropy production of the sample is then given by Eq. (10), derived from Eqs. (6)–(9), which describes, besides fusion or crystallization, also changes in lamellar thickness, dl.

The easiest use of Eq. (10) is for sufficiently large crystals (case 1 in Fig. 14). All terms with ↕ in the denominator can then be neglected. Equilibrium melting and crystallization occurs when Δg_f is zero and produces zero entropy production since the entire change in entropy is provided by flux. Crystallization with supercooling is irreversible ($\Delta T > 0$, $dm_c > 0$). The same is true for melting with superheating ($\Delta T < 0$, $dm_c < 0$). Note that Δh_f is always endothermic (+). In contrast, crystallization with superheating and melting with supercooling violate the second law.

Case 2 in Fig. 14 allows the discussion of thin lamellae. In case no melting occurs ($dm_c = 0$), only an increase in lamellar thickness ($dl > 0$) is allowed under the given conditions. Assuming no change in thickness ($dl = 0$), melting and crystallization is allowed by the second law above and below a special, second zero-entropy-production temperature, respectively. This *zero-entropy-production temperature* is defined for thin crystals when the two melting terms compensate with $dm_c \neq 0$, which means that the melt and the crystal must have the same metastability. The three other processes, decreasing in thickness without an overcompensating melting term in Eq. (10), melting below, and crystallization above the zero-entropy-production temperature, are forbidden since they would lead to a negative entropy production.

On the one hand, Fig. 14 allows the development of descriptions of the melting of metastable, small systems, but on the other, it also indicates the large number of conditions that must hold in order to get to a simple equation. The cases listed with entropy production ($d_i S > 0$) can only be handled if the free enthalpy of the involved metastable states can be derived separately and inserted in Fig. 13, as illustrated in Fig. 2 for polyethylene where ↕ was determined separately. The condition to keep ↕ constant during melting, points to the advantage to bypass reorganization with fast melting of small samples, a topic which developed to major importance as discussed during the Seventh and Eighth Lähnwitz Seminars and displayed in [2] and elsewhere in this issue. It is also summarized in [33]. Besides using fast thermal analysis, fixing the nanophase structure to a constant ↕ by chemical cross-linking or by removing the amorphous subsystems with chemical etching were developed in the 1970s [16] and should also be applicable for thin-film analysis.

6. Conclusions

It is shown that sufficiently thin films reach microphase or nanophase dimensions. For polymers, even externally macroscopic samples contain such small phases. Frequently these small systems are metastable and need nonequilibrium thermodynamics for their description. Besides the surface effects caused by the size restriction, strains across interfaces are common in macromolecular systems and must be considered as they lead to broadened glass transitions and separate rigid–amorphous nanophases. Metastable systems may become unstable on heating and reorganize during analysis. Analyzing nanogram samples with super-fast heating rates, which have recently reached as high as 10^6 K min^{-1} [2,33], may allow to bypass reorganization in thermal analysis.

Acknowledgments

This work was supported by the Division of Materials Research, National Science Foundation, Polymers Program, Grant # DMR-0312233. Use of some of equipment and laboratory space was provided by the Division of Materials Sciences and Engineering, Office of Basic Energy Sciences, U.S. Department of Energy at Oak Ridge National Laboratory, managed and operated by UT-Battelle, LLC, for the U.S. Department of Energy, under contract number DOE-AC05-00OR22725.

References

[1] C. Schick, U. Rostock, F. Physik, A. Polymerphysik, G.W.H. Höhne, Gesellschaft für Thermische Analyse e.V. (GEFTA), Arbeitskreis Kalorimetrie, Biannual Meetings since 1990.
[2] Published in sequence in: Thermochim. Acta 304/305 (1997), 330 (1999), 377 (2001), 403 (2003), and the present issue.
[3] G. Tammann, Z. Anorg. Allg. Chemie 111 (1920) 166.
[4] F. Meissner, Z. Anorg. Allg. Chemie 111 (1920) 169.
[5] H.A. Stuart, Die Physik der Hochpolymeren, vols. 1–4, Springer-Verlag, Berlin, 1952–1956.
[6] B. Wunderlich, Polymer 5 (1964) 125 and 611.
[7] B.G. Sumpter, D.W. Noid, G.L. Liang, B. Wunderlich, Adv. Polym. Sci. 116 (1994) 27.
[8] J.-U. Sommer, G. Reiter, Thermochim. Acta, elsewhere in this issue.
[9] L. Zhu, S.Z.D. Cheng, S.L. Thomas, B. Lotz, J. Am. Chem. Soc. 122 (2000) 5957.
[10] H. Suzuki, J. Grebowicz, B. Wunderlich, Br. Polym. J. 17 (1985) 1.
[11] S.N. Magonov, N.A. Yerina, G. Ungar, D.H. Reneker, D.A. Ivanov, Macromolecules 36 (2003) 5637.
[12] J.A. Morrison, L.E. Drain, J. Chem. Phys. 19 (1951) 1063.
[13] Y. Fu, W. Chen, M. Pyda, D. Londono, B. Annis, A. Boller, A. Habenschuss, J. Cheng, B. Wunderlich, J. Macromol. Sci. Phys. B 35 (1996) 37.
[14] B. Wunderlich, Thermochim. Acta 403 (2003) 1.
[15] J.W. Gibbs, Am. J. Sci. Ser. 3 (16) (1878) 441.
[16] B. Wunderlich, Macromolecular Physics, vol. 1: Crystal Structure, Morphology, Defects, Academic Press, New York, 1973;
B. Wunderlich, Macromolecular Physics, vol. 2: Crystal Nucleation, Growth, Annealing, Academic Press, New York, 1977;
B. Wunderlich, Macromolecular Physics, vol. 3: Crystal Melting, Academic Press, New York, 1980.
[17] J.A. Morrison, L.E. Drain, J. Chem. Phys. 19 (1951) 1063.
[18] J. Pak, B. Wunderlich, Macromolecules 34 (2001) 4492.
[19] H. Kraack, M. Deutsch, E.B. Sirota, Macromolecules 33 (2000) 6174.
[20] U. Gaur, B. Wunderlich, Macromolecules 13 (1980) 1618.
[21] J.A. Forrest, J. Mattsson, Phys. Rev. E 61 (2000) R53.
[22] S.A. Adamovsky, A.A. Minakov, C. Schick, Thermochim. Acta 403 (2003) 55.
[23] H. Huth, A.A. Minakov, C. Schick, in: M.J. Rich (Ed.), Proceedings of the 32nd NATAS Conference, vol. 32, Williamsburg, VA, October 4–6, 2004, MS 166-05_384_A (CD edition).
[24] H. Bu, E. Chen, S. Xu, K. Guo, B. Wunderlich, J. Polym. Sci., Part B: Polym. Phys. 32 (1994) 1351;
B. Lotz, A.J. Kovacs, G.A. Bassett, A. Keller, Kolloid Z. Z. Polymere 209 (1966) 115.
[25] M.L. Di Lorenzo, M. Pyda, B. Wunderlich, J. Polym. Sci., Part B: Polym. Phys. 39 (2001) 1594, 2969.
[26] Y.K. Kwon, A. Boller, M. Pyda, B. Wunderlich, Polymer 41 (2000) 6237.
[27] M. Pyda, E. Nowak-Pyda, J. Mays, B. Wunderlich, J. Polym. Sci., Part B: Polym. Phys. 42 (2004) 4401.
[28] J. Pak, M. Pyda, B. Wunderlich, Macromolecules 36 (2003) 495.
[29] P.J. Flory, Principles of Polymer Chemistry, Cornell University Press, Ithaca, 1953, and later editions.
[30] See for example: L. Mandelkern, Crystallization of Polymers, 2nd ed., Cambridge University Press, 2004.
[31] B. Wunderlich, Thermal Analysis of Polymeric Materials, Springer-Verlag, Berlin, 2005, 894 + xvi pages, 947 figures.
[32] I. Prigogine, Introduction to the Thermodynamics of Irreversible Processes, 2nd ed., Interscience, New York, 1961.
[33] B. Wunderlich, Fast and super-fast DTA and calorimetry, in: Proceedings of the 32nd NATAS Conference, vol. 32, Williamsburg, 529 VA, 2004, MS 018-04 569 P, 10 pp. (CD edition); J. Therm. Anal. Calorimetry, 2005, in press.